ELSEVIER

Journal of Alloys and Compounds 223 (1995) 226–236

Journal of ALLOYS AND COMPOUNDS

The magnetism of localized or nearly localized 4f and 5f shells

O. Vogt, K. Mattenberger

Institut für Festkörperphysik, ETHZ, Hönggerberg, CH-8093 Zürich, Switzerland

Abstract

The magnetic properties of monopnictides and monochalcogenides of both the rare earths and the actinides are discussed. All these compounds crystallize in the NaCl type of structure where interatomic distances are large. The electrons of the 4f or 5f shells should therefore be reasonably localized in these mostly trivalent, partially ionic compounds. Macroscopic magnetic properties are governed by crystal field interaction, isotropic and anisotropic exchange forces and hybridization of the f electrons. Differences between the magnetic properties of 4f and 5f compounds are due to the relative importance of the above-mentioned parameters. They strongly depend on the spatial extension of the f electrons, which is significantly more important in the case of the actinides.

Keywords: Magnetism; Monopnictides; Monochalcogenides

1. Introduction

Magnetic phenomena are traditionally explained either by an itinerant electron model or by taking discrete localized electron orbits into consideration. Usually f electrons are treated as being localized, but in many compounds strong interactions with s, p and d electrons cannot be overlooked. Historically magnetochemistry, using the paramagnetic properties of partially filled 4f and 5f shells, was a powerful analytical tool. Assuming a Russell–Saunders coupling, the valency of an f ion can be determined under the condition that within a reasonable temperature range the Curie–Weiss law is obeyed. Of course, valences obtained by this procedure have to be compatible with results gained by comparison of lattice parameters. For instance, anomalously large atomic volumes of Yb and Eu are the consequence of the divalency of the f shells.

Self-consistent-field calculations for free ions show that 5f electrons are of a larger spatial extent than 4f electrons, less shielded by outer electrons and more easily removed from the atom. These facts are mainly responsible for the differences encountered in the magnetic behaviour of 4f and 5f compounds (or elements). For instance, the light actinide metals are all non-magnetic owing to strong hybridization of their f electrons. In ionic actinide compounds there seems to be a critical interatomic distance (Hill limit) above which localized (in real and energy space) behaviour can be expected. Such a limit would be much lower for rare-earth compounds.

Monopnictides and monochalcogenides with the simple cubic NaCl structure exist with only a few exceptions for all the rare earth and actinide elements. They are of the simple formula (Ln,An)X, X=N, P, As, Sb, Bi or O, S, Se, Te. With increasing atomic number the f shells become smaller and thus more localized, i.e. the bandwidth becomes very small. On the other hand, on going to the heavier anions (i.e. from N to Bi or from O to Te) the interatomic distance increases and this favours localized (free-ion like) moment behaviour. The limited small number of hybridizing anion p electrons is favourable for theoretical calculations.

The miscibility of most of the chalcogenides and pnictides opens up the attractive possibility of "tailoring" model substances: by replacing the actinide or rare earth ion with "non-magnetic" (no partially filled f shell) ions, i.e. La, Th, Lu or Y, we can weaken the exchange forces (keeping crystal field and hybridization constant), and by replacing the pnictogen with the chalcogen, we can gradually (up to one) increase the number of hybridizing p electrons.

The spatial distribution and the degree of energy overlap are decisive for the magnetic behaviour, which is either of the localized-moment type or band-like magnetism. In addition to shifting the energy bands, hybridization manifests itself in two other phenomena, anisotropic exchange forces and a moment wash out. We shall discuss later its influence on the crystal electric field (CEF) splitting.

A suitable disposition of the Periodic Table (after Smith and Kmetko [1]) (Fig. 1) illustrates clearly the

0925-8388/95/$09.50
SSDI 0925-8388(94)09005-X

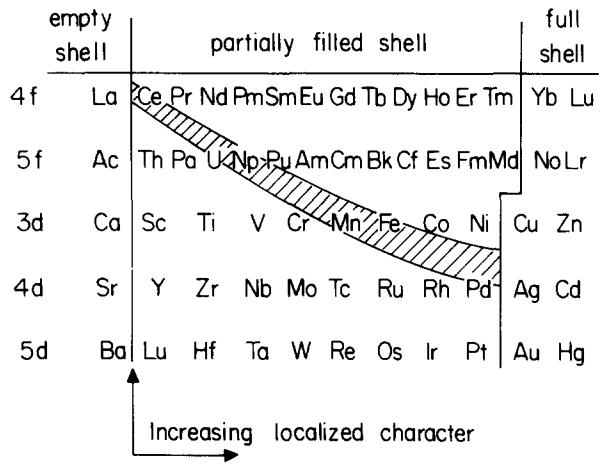

Fig. 1. Table of the elements of the 3d, 4d, 5d, 4f and 5f series arranged in an order showing the systematic variation of the localized character among the partly filled d and f shells (after Smith and Kmetko [1]).

situation for rare earth and actinide compounds. Often one talks, especially in discussions of U compounds, about "rare earth-like" behaviour and means by "rare earths" the elements past Gd. This does not make much sense. U compounds should be compared with Nd compounds, where signs of delocalization are also clearly visible! The hatched area in Fig. 1 marks the critical region for the metals where the transition from magnetism to superconductivity occurs. We can expect "irregularities" in the compounds which occur in the vicinity of this area.

2. Rare earth and actinide ions in a crystalline matrix

2.1. Spectroscopic ground state: valency

The bonding in NaCl-type compounds is at least partially ionic. The valency of the rare earth or actinide ion, and thus the spectroscopic ground state, are usually determined by comparing the lattice parameter of a compound with similar compounds of the other cations or simply by relying on the published values for the ionic radii. Magnetization measurements, i.e. comparing measured effective moments with theoretical values based on Russell–Saunders coupling, provide another strong indication for the true valence state. The isomer shift in Mössbauer experiments is, whenever possible, the most reliable experimental method to determine the valency.

The rare earth ions in pnictides and chalcogenides are usually in the trivalent state. There are some significant exceptions, however: Eu in its chalcogenides is divalent, the Sm chalcogenides are of intermediate valency and TmSe is a mixed-valent system, the same as CeN and probably the Nd chalcogenides. Yb pnictides are trivalent at room temperature and change to heavy-fermion behaviour at low temperatures [2]. The Yb chalcogenides are all divalent. We realize that divalency in rare earth compounds is encountered in chalcogenides only.

The actinide elements form compounds with usually three to five different valence states. In the rock salt structure, however, we find almost exclusively trivalent cations. Th is always tetravalent. In some U chalcogenides tetravalency cannot be excluded. The Pu chalcogenides might be mixed-valent (2.75) compounds [3]. From Pu on there are no more exceptions from trivalency (cf., e.g., magnetic susceptibility measurements on Cf pnictides [4]). Russell–Saunders coupling with moderate J mixing in some cases, describes the experimental findings fairly well.

2.2. The crystal electric field (CEF)

The crystal electric field will always be present, although it may be very weak and hard to detect. The ground state of the multiplet and higher terms also are split. It should be possible to estimate the strength of an unshielded crystal field by an electron point charge model (EPCM). According to this simple model, the crystal field should be proportional to a^5 (a = lattice parameter). This holds for light rare earth NaCl-type compounds, as can be seen in Fig. 2 [5].

The heavy rare earth compounds do not follow the a^5 law and values for Ce pnictides are well below the pattern. Crystal field splittings can be determined by various kinds of inelastic neutron scattering experiments, by specific heat measurements (Schottky anomalies), by Mössbauer studies or by fitting magnetization measurements.

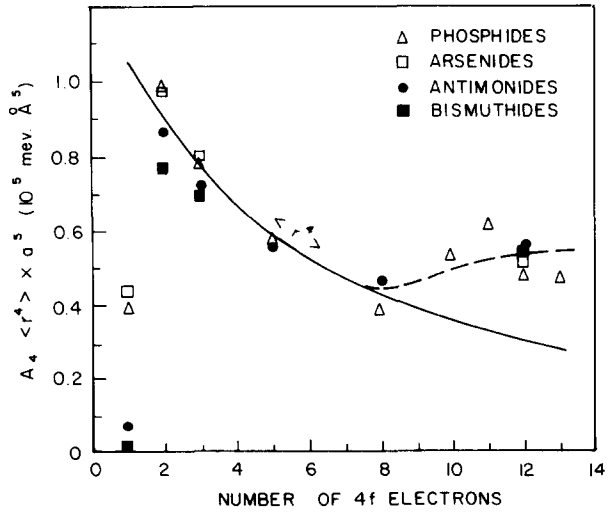

Fig. 2. Fourth-order crystal-field parameter times the lattice constant a raised to the fifth power in number of rare-earth monopnictides. The solid line is the EPCM prediction with $Z_e = 1.2$ and r^4 equal to the Dirac–Slater values calculated by Lewis.

For the actinide compounds, however, it was possible in only a very few cases to identify the crystal fields unambiguously. In USb and UTe this is due to the fact that exchange forces, which are much higher in actinides than in rare earths, and hybridization obscure the crystal field levels [6,7].

The EPCM model apparently does not hold for Ce compounds and for actinide compounds. Kasuya's group offered a very convincing explanation for this discrepancy by taking hybridization with p electrons into account. This leads to an "effective crystal field". The symmetry conditions for the level splitting remain valid. Fig. 3 shows splittings due to the "effective" CEF in CeSb–CeTe mixed crystals [8]. A clear dependence on the (excess) p electron concentration is obvious.

In magnetic properties, we can roughly observe two different phenomena: at low temperatures the observed ordered moment may be only due to the lowest CEF level (e.g. in CeP) and at higher temperatures Van Vleck-type paramagnetism of the CEF levels is observed.

2.3. Exchange

Exchange forces can be isotropic or anisotropic. Isotropic exchange of the Heisenberg type by direct overlap of f electrons is not probable. We must consider super-exchange, such as is encountered in (insulating) Eu chalcogenides. In metallic compounds there is the possibility of isotropic RKKY exchange. The sign of exchange can change as a function of distance both for Heisenberg-type and for the more familiar oscillatory RKKY exchange. We are never entitled to conclude that exchange is of the RKKY type just because it changes sign with increasing interatomic distance; see, e.g., arguments given on the magnetic properties of Cm pnictides in Ref. [9].

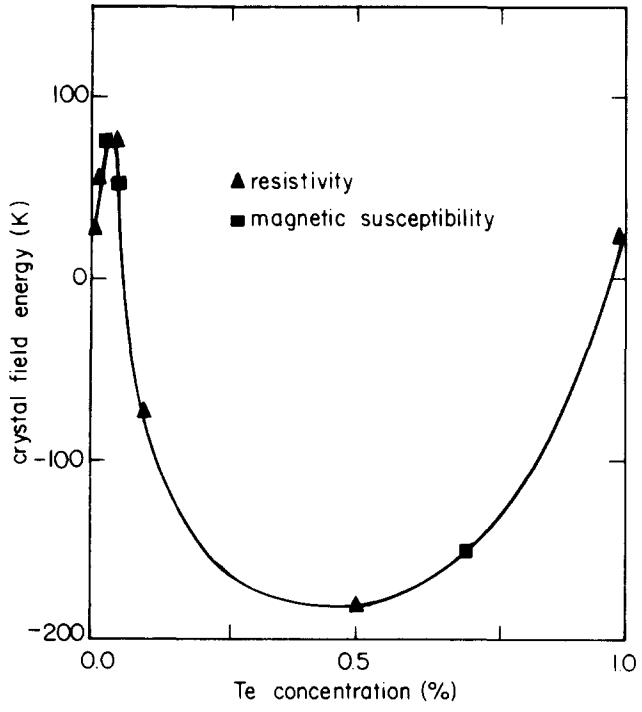

Fig. 3. Crystal field splitting energy $\Delta = E(\Gamma_8) - E(\Gamma_7)$ as a function of x in $CeSb_{1-x}Te_x$, deduced from magnetic susceptibility measurements (■) and resistivity measurements (▲) as explained in the text.

Anisotropic exchange can be caused by single-ion anisotropy, i.e. the ion is reshaped either by CEF interaction or by hybridization. The response to an applied or internal field depends on its orientation. Trammell [10] has shown that, under the assumption of isotropic exchange, the magnetic axes are determined by the CEF. Reshaping of the single ions by hybridization has a twofold influence on the magnetic properties: exchange interactions depend on the crystalline orientation and the single-ion moment can be "washed out" or reduced by the loss of electrons in real and energy space due to bonding [11].

Anisotropic two-ion interactions are due to hybridizing p and d electrons. Calculations of the sign and spatial distribution of anisotropic exchange are very difficult. Experimental evidence of the existence of anisotropic exchange can often be found. Thus, if in a compound the easy axis is not the one preferred by the CEF interaction, we can be sure that exchange is anisotropic. This is true, e.g., for CeSb. In favourable cases Mössbauer spectroscopy on ^{121}Sb can put an f and p anion hybridization in evidence, which gives rise to anisotropic exchange (28a,b) [12,13]. Exchange can be directly "seen" by neutron diffraction. Finally, neutrons have revealed a multitude of interesting spin structures. In NaCl-type crystals, isotropic exchange can lead only to ferromagnetism or antiferromagnetism of type I, II or III. All other spin structures are clear evidence for anisotropic exchange.

3. Magnetic susceptibilities

We shall consider true susceptibilities in the paramagnetic state, i.e. the ratio of magnetization versus magnetic field in the limit of zero applied field. In cubic systems these susceptibilities should be isotropic above the ordering temperatures. If they are not, some long-range order must be present. In the ordered state susceptibilities depend, as a rule, on the orientation of the applied field. Domain effects can render the determination of low-field susceptibilities questionable.

Traditionally, measured inverse susceptibilities are plotted versus temperature. The usually obtained straight relationship can be fitted by a Curie–Weiss law. The effective number of magnetons is compared with the calculated free-ion value. Usually, the non-4f contributions to $\chi(T)$ can be neglected. In certain cases, however, a relatively large temperature-independent term χ_0 has to be added to the Curie–Weiss term, i.e.

measured susceptibilities χ_m seem to follow a "modified Curie–Weiss law":

$$\chi_m = \chi_{cw} + \chi_0$$

Very little is known about the origin of this term χ_0.

A sample dependence is obvious. Recent χ measurements on PuSb [14] yield $\chi_0 = 30 \times 10^{-10}$ emu mol^{-1}, whereas old measurements were interpreted with a value of 200×10^{-6} emu mol^{-1} [15]! Similar findings are reported for PuP [16]; here the χ_0 value could be due to strain-induced magnetic moments.

A logical explanation for the occurrence of χ_0 is found in the mixed system US–ThS where the observed value of χ_0 is actually due to the susceptibility of ThS, which is 32×10^{-6} emu mol^{-1}, a surprisingly high value [17].

In another mixed system, PuSb–PuTe, the observed χ_0 values correspond to the concentration of PuTe, which in the pure state reveals a temperature-independent paramagnetism [18]. Paramagnetic susceptibilities of the non-ordering actinide metals are very high, of the order $(200–600) \times 10^{-6}$ emu mol^{-1}. Large values are even observed in rock salt-type americium compounds [9], in contradiction to the $J=0$ ground state of the Am^{3+} ion.

Explanations are offered either by enhanced Pauli paramagnetism (some compounds are heavy-electron systems) or by Van Vleck-type mixing of CEF terms. Calculations of the susceptibilities of SmS (Sm is divalent with $J=0$) taking crystal field terms into account [19] or, more elaborately, exchange terms between CEF levels in addition [20] show that at zero temperature a value of the order 300×10^{-6} emu mol^{-1} seems to persist.

J mixing explains the magnetic properties of Sm^{2+} chalcogenides at high temperatures [21]. At low temperatures an admixture of 3% Sm^{3+} ions is postulated. A similar model [3] could explain the behaviour of the Pu chalcogenides; Pu should be in a 2.75 valence state.

In favourable cases, i.e. if exchange forces are not too strong and hybridization is not predominant, the low-temperature susceptibilities can be explicitly calculated based on a CEF splitting model.

The ground state of Tm^{3+} in TmSb is a singlet, and thus non-magnetic [22]. Based on this model, the experimental susceptibilities are very well explained, as is evident in Fig. 4.

Exchange is completely absent, since dilution with 50% non-magnetic YSb has no influence on the susceptibilities [23]. Moderate exchange would shift the curves upwards as in the case of TbSb–YSb mixed crystals [24]. The Tb^{3+} ground state is also a singlet. The behaviour found for diluted UTe [25] is very reminiscent of results obtained on diluted TbSb. Unfortunately, a reliable value of the overall splitting is not yet available.

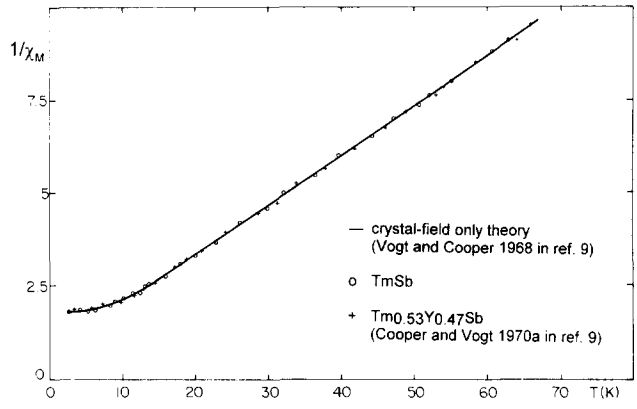

Fig. 4. Inverse susceptibility of TmSb (open circles) and $Tm_{0.53}Y_{0.47}Sb$ (crosses) vs. temperature. The solid line is the calculated crystal-field only theory.

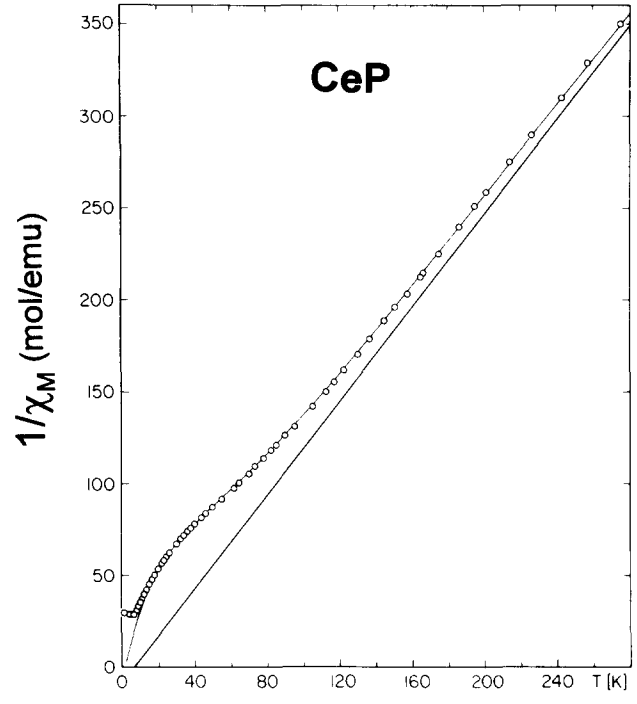

Fig. 5. Inverse magnetic susceptibility of CeP. The curve approximating the measured points (circles) is calculated. The straight line represents the underlying Curie–Weiss law.

Calculations of the susceptibility of CeP were the first examples for a compound with a doublet (magnetic) ground state [26] (Fig. 5). Again, the experimental values are very well represented by calculations. These results were further refined by taking interlevel exchange into account [27].

As a general rule, flattening out of the Curie–Weiss curve is an indication of a non-magnetic CEF ground term whereas a magnetic term manifests itself with a downturn towards low temperatures. Susceptibilities below ordering temperatures show a very complex behaviour: for a ferromagnet or an isotropic antiferromagnet the susceptibility should remain constant below the ordering temperature. For a uniaxial antiferro-

magnet we expect a constant perpendicular and a vanishing parallel susceptibility. Occasionally an enormous upturn of the inverse susceptibility is observed (e.g. in Dy or Ho pnictides) [28] following none of the above-mentioned rules.

In an intermediate temperature range (usually up to 300 K), the Curie–Weiss law is followed. Very useful information can be obtained even for microgram samples. Let us cite in this connection measurements on Cf pnictides [4], which reveal trivalency of the Cf ion, allow an estimation of the CEF and define the ordering temperatures.

If we meet an important deviation of the experimental magneton numbers compared with the free-ion Russell–Saunders coupling calculations, we have to look for its reasons: valence changes, J mixing, CEF interaction or hybridization dressing of the ions are the most frequently studied options. Such deviations occur preferentially near both ends of the lanthanide or actinide series.

At high temperatures we expect to see a Van Vleck-type paramagnetism (J mixing). Unfortunately, susceptibility measurements at high temperature are scarce. For lanthanides their importance was probably underestimated and for actinides safety problems are one reason for their absence. Old measurements on Nd chalcogenides [29] are shown in Fig. 6.

It is evident that by choosing an appropriate screening factor, theory describes the experimental findings very well. Recently, we carried out high-temperature measurements on the U chalcogenides (both Nd and U have the same number of f electrons). The resemblance is striking (Fig. 7). It is hoped that a careful analysis

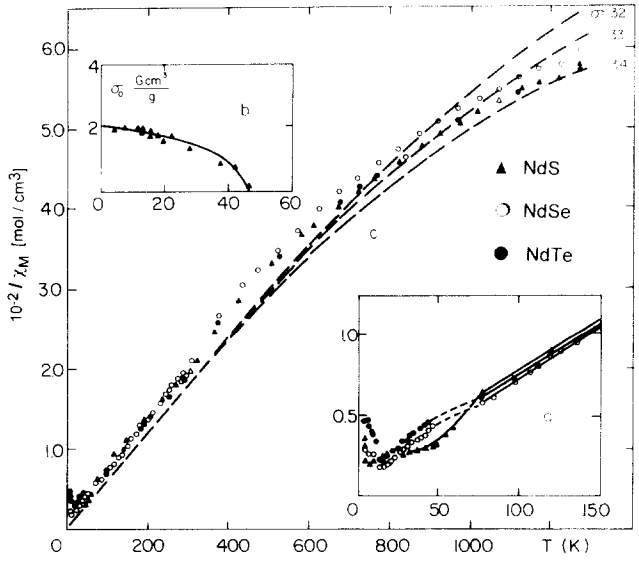

Fig. 6. Inverse molar susceptibilities vs. temperature for NdS, NdSe and NdTe. Broken lines are calculated Van Vleck susceptibilities for various screening factors ($\sigma = 32, 33, 34$).

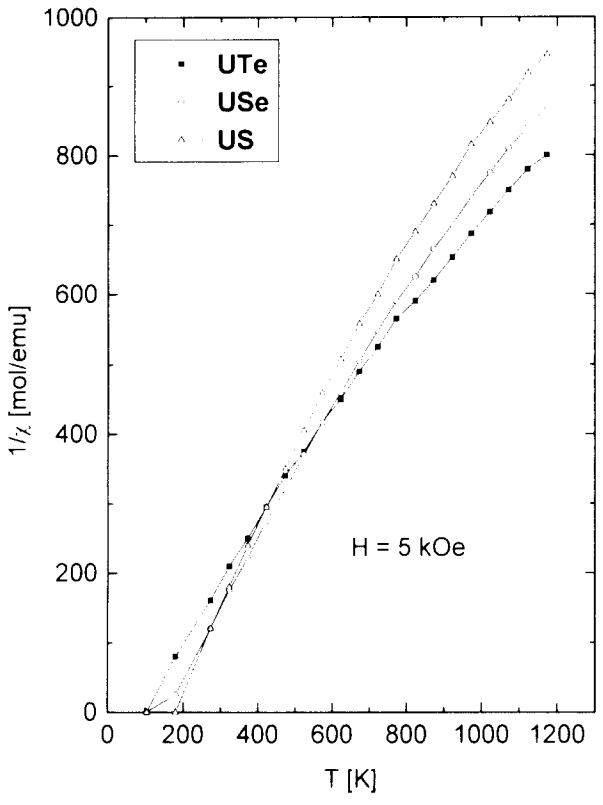

Fig. 7. Inverse molar susceptibilities of uranium monochalcogenides versus temperature.

will yield valuable information on the ionicity of U in the monochalcogenides and on the effective CEF.

As we have seen, susceptibility curves will always have to be analysed by taking CEF, J mixing and the Curie–Weiss-type mechanism into account. We have schematically considered three temperature regions: low temperature (CEF), intermediate temperature (Curie–Weiss) and high temperature (J mixing or mixing of CEF states). The onset of order is the lower limit for these experiments and the melting point is the upper limit.

4. Magnetization

Measurements of the magnetization at low temperature are performed in order to gain information about the magnitude of ordered moments and the easy axes. Since magnetizations are anisotropic for almost all the lanthanide and actinide compounds (exceptions are Cm, Gd and Eu compounds where the ions have an "S" ground state), reliable measurements always have to be done on single crystals.

In a true ferromagnet, the magnetization corresponds directly to the magnetic moment of the f electrons. Practically all the antiferromagnetic compounds can be turned into ferro- or ferrimagnets by the application of high magnetic fields (about 100 kOe). If the spin

structures of the induced phases are known (or can be guessed), it is possible to determine atomic moments; these moments, however, are not necessarily the "spontaneous" moments but may be significantly increased by the relatively high applied external fields. Thus, in most cases, only neutron diffraction experiments provide reliable information on the size of the zero-field ordered 4f or 5f moment. The anisotropic behaviour can be safely determined by magnetization measurements.

Magnetization measurements in a fixed external field as a function of temperature give some more information. Comparing such results with theoretical curves based on the Brillouin function is a useful method to judge the ground state of the magnetic ion. In favourable cases, when CEF and exchange are not of equal importance, a theoretical analysis of magnetization curves becomes possible.

If exchange is absent or very weak, the response of the ion to an external field can be calculated based on the CEF splitting. Such calculations have been done for TmSb [22,23] and are shown in Fig. 8.

The most remarkable fact is the anisotropy, which is apparently induced by an external field. This CEF anisotropy is one reason for the generally observed bulk anisotropy. Trammell [10] calculated as early as 1963 that, under the assumption of isotropic (or very weak) exchange, the magnetic (easy) axis is determined by the CEF splitting. In the case of TbSb, like TmSb a singlet ground-state system, exchange forces are moderate and can be overcome (see Fig. 9) by an external field [24]. By diluting TbSb with YSb one can get rid of exchange completely and we obtain the same magnetization curves as in TmSb [25].

In the cases of CeAs and CeP [26], the CEF influence is much stronger than exchange or external field. The observed low-temperature magnetization, even at 200 kOe, corresponds to the moment of the CEF ground

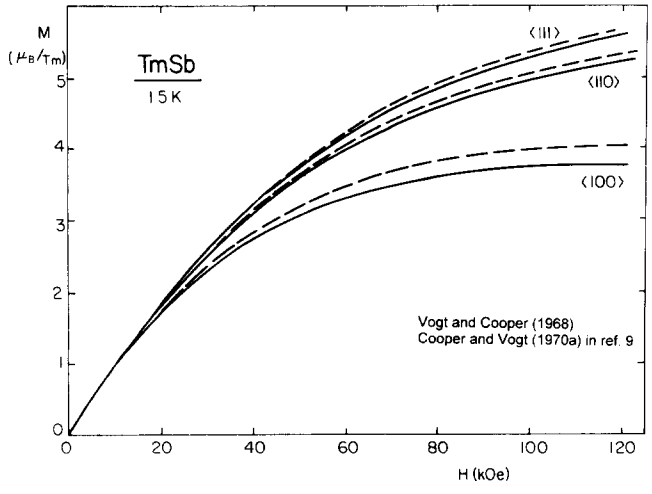

Fig. 8. Magnetization vs. applied field at 1.5 K of TmSb. Solid lines are experimental results and dashed lines are calculated curves.

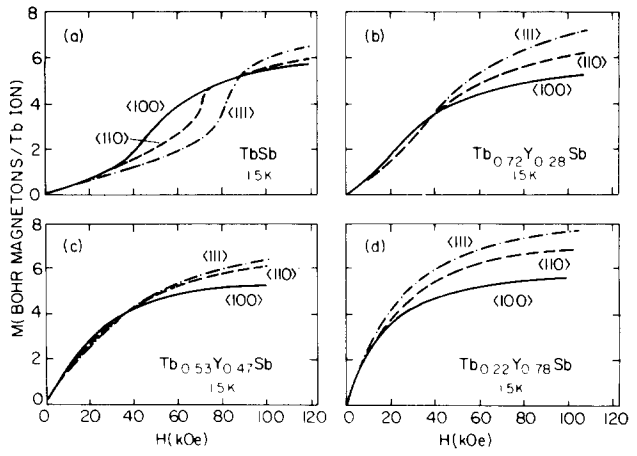

Fig. 9. Magnetization per Tb ion for $Tb_xY_{1-x}Sb$ at 1.5 K.

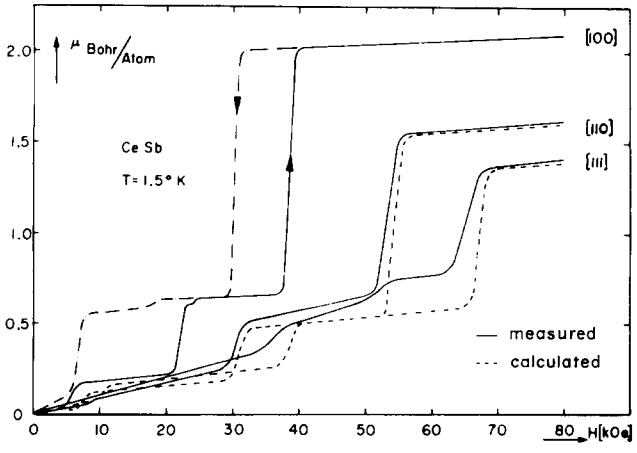

Fig. 10. Magnetic moments of CeSb at 1.5 K, measured in external fields along the ⟨100⟩, ⟨110⟩ and ⟨111⟩ axes.

state and is much lower than the free-ion value. Strong anisotropic exchange may rule out CEF anisotropy. In ordered CeSb [30] (Fig. 10) we observe clearly a ⟨100⟩ easy axis and a full ionic moment. Calculations based on CEF theory would yield ⟨111⟩ as the easy axis, and this is indeed observed in heavily diluted CeSb, i.e. in the compounds $Ce_{0.1}Y_{0.9}Sb$ or $Ce_{0.1}La_{0.9}Sb$ [31]. The observed magnetic axis, in the case of CeSb, is thus due to anisotropy of the exchange interactions and not to CEF interaction.

Competition of CEF and exchange anisotropy can lead to very complicated spin structures, e.g. in the case of the Ho pnictides [53] or CeSb and CeBi and also in U, Np and Pu monopnictides. In some cases, an external field can induce a multitude of stable spin structures, as is seen in Fig. 11 [32].

The macroscopic and microscopic behaviour of such compounds has to be described by magnetic phase diagrams, i.e. by dividing up the H, T space into regions of different spin structures. These diagrams are usually obtained by combining the results of magnetization and neutron diffraction experiments.

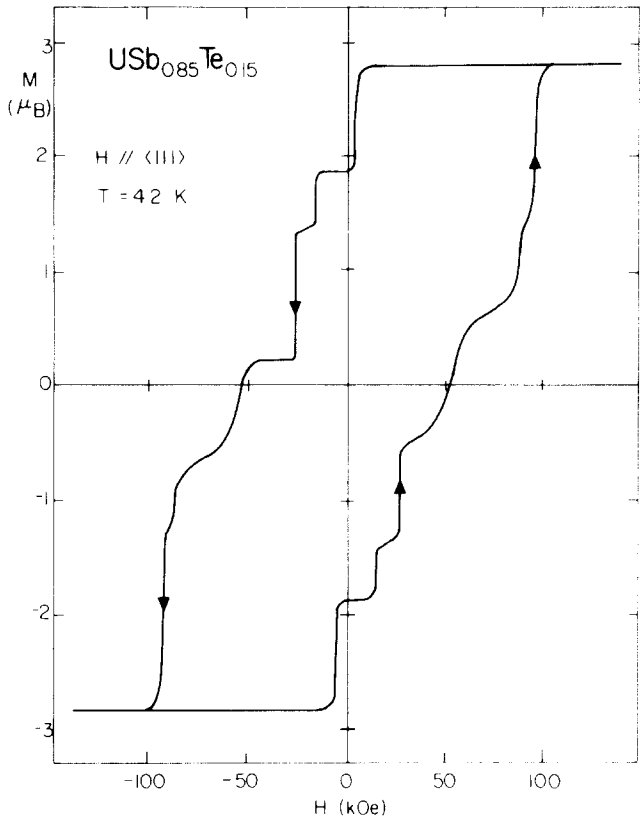

Fig. 11. Hysteresis loop at $T = 4.2$ K of $USb_{0.85}Te_{0.15}$.

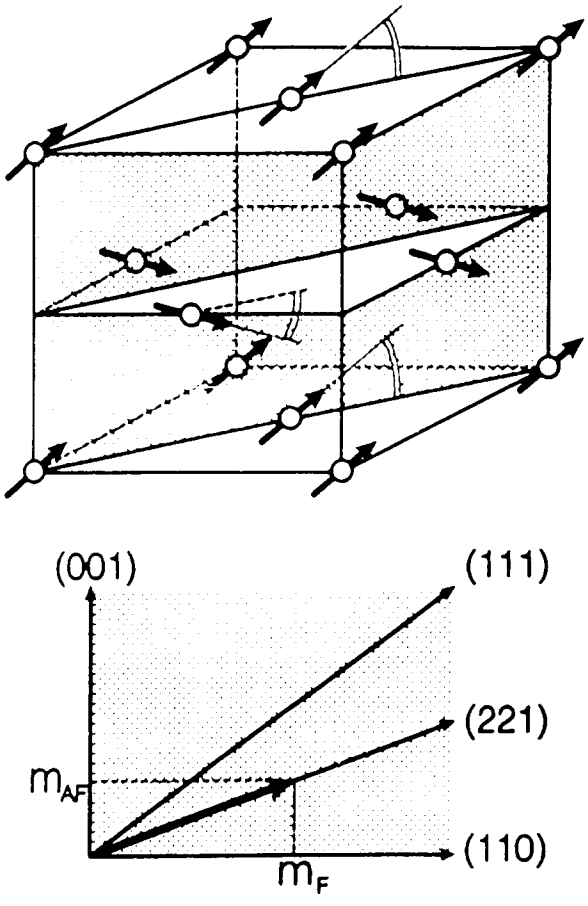

Fig. 12. Non-collinear ferrimagnetic structure of $NpSb_{0.95}Te_{0.05}$.

5. Spin structures

It can be shown that under the assumption of isotropic exchange, restricted to nearest and next-nearest neighbours, only antiferromagnetism type I, II and III or ferromagnetism are possible in an ionic fcc lattice [33]. In both actinide and rare earth compounds of the NaCl structure, we find, however, a multitude of different spin structures. This is a clear indication that in these compounds exchange is anisotropic, due either to hybridization-mediated reshaping of the single ions or to an anisotropic exchange mechanism.

Unusual spin structures in rare earth compounds are the ferrimagnetic structures found for some nitrides [34], the peculiar HoP structure [34] encountered also in some Dy compounds. Spin structures found in ErN and NdS were very mysterious for a long time.

Further progress stems from the intensive work by the late Jean Rossat-Mignod and his group in Grenoble, France, on Ce and actinide compounds of the NaCl-type structure. Let us mention the magnetic phase diagram of CeSb, which at first sight looks extremely complicated [35]. The simple concept of "paramagnetic planes" renders its interpretation very plausible: the spins in CeSb are ferromagnetically arranged in [100] planes, which are stacked along ⟨001⟩. Intraplanar exchange is much stronger than exchange between the [100] planes. Thus it is possible that some planes are in a frustrated state, probably oscillating between "up" and "down", and manifesting themselves as "paramagnetic planes". All spin structures encountered in CeSb can be readily explained by commensurate sequences of "up"', "down" and paramagnetic planes.

Other new spin arrangements were found in the multi-k structures of certain uranium compounds [36]. They explained many mysteries, e.g. the absence of lattice distortions in some antiferromagnetic U compounds. For UP a moment jump was observed at 22.5 K by neutron diffraction. This moment jump did not seem to be coupled to any structure change. It is explained by the transition of 1 k to 2 k antiferromagnetism, both of which show identical neutron diffraction patterns [37].

Today we know that the Fourier components of the magnetization vector not only exist independently of each other, ordered ferro- or antiferromagnetically, but that the coexistence of ferromagnetic and antiferromagnetic arrangements is also possible. The three components of such non-collinear structures need not have the same magnitude. One example is the ferrimagnetic spin structure found in $NpAs_{0.95}Se_{0.05}$ [38].

With today's knowledge about multi-k structures, all the above-mentioned mysterious spin structures en-

countered in rare earth compounds can probably be easily explained [9].

6. Conclusions

We have shown that magnetic properties depend on a delicate equilibrium between CEF interaction, anisotropic exchange and hybridization-mediated reshaping of the ions, the last two being more important in actinide compounds since the 5f electrons are more delocalized in real and energy space than 4f electrons. By magnetic dilution we can weaken the exchange forces (which are generally stronger in actinides) and obtain a magnetic behaviour in actinide compounds which is absolutely homologous with that in their rare earth counterparts. By mixing pnictogens and chalcogens it is possible to influence hybridization.

Appendix

Tables A1 and A2 summarize today's knowledge of the magnetic properties of rare earth and actinide monopnictides and monochalcogenides.

Table A1
Magnetic properties of ordering trivalent rare-earth monopnictides and monochalcogenides [a]

Compound	a (Å)	Magnetism	$T_{crit.}$ (K)	θ_{para} (K)	$\mu_{eff.}$ (μB)	$\mu_{neut.}$ (μB)	$\mu_{sat.}$ (μB)	Easy axis
CeN	5.023	m.v. n.o.						
CeP	5.909	AF I?	8.5	5	2.56		0.85	⟨100⟩
		AF I 3k?						⟨111⟩
CeAs	6.07	AF I?	7.5	18	2.82		0.85	⟨100⟩
		AF I 3k?						⟨111⟩
CeSb	6.412	Many phases	16.2	5	2.56		2.08	⟨100⟩
CeBi	6.500	AF I/AF IA	25.5/12.5	12	2.38		2.1	⟨100⟩
CeS	5.763	AF II	8.3	−20	2.78		0.57	⟨111⟩
CeSe	5.992	AF II	5.4	−7	2.58		0.58	⟨111⟩
CeTe	6.359	AF II	2.2	−4	2.49		0.3	⟨111⟩
NdN	5.151	Ferro	27.6	24	3.65	2.69	3.6	
NdP	5.838	AF I	11	11	3.78	1.83	2.2	
NdAS	5.970	AF I	10.6	4	3.7	2.18	2.3	⟨100⟩
NdSb	6.322	AF I	15.5	−3	3.75	2.98	2.7	⟨100⟩
NdBi	6.424	AF I	25	−1	3.58	3.1		⟨100⟩
NdS	5.691	AF n.c. AF II	8.2	−26.5	3.62	1.9	2.24	24° off ⟨111⟩
NdSe	5.909	AF II	10.6	−9	3.52	1.57	2.34	⟨111⟩
NdTe	6.262	AF II	10.2	−14	3.54	1.1	2.58	⟨111⟩
GdN	4.999	Ferro	72	69	8.15		7.03	
GdP	5.723	AF	20	0	7.94		7.1	
GdAs	5.861	AF	21	−12	7.96		7.25	
GdSb	6.217	AF II	28	−42	8.1			
GdBi	6.316	AF II	32	−65	8.03			
GdS	5.574	AF II	62	−104	8.16			
GdSe	5.781	AF II	65	−110	8.23			
GdTe	6.139	AF ?	70	−90	7.94			
TbN	4.933	Ferro	42/34	34	10	6.7/7		⟨111⟩
TbP	5.688	AF II	9	3	9.2	6.2		⟨111⟩
TbAs	5.827	AF II	12	−4	9.6	7.7		⟨111⟩
TbSb	6.170	AF II	14/16.5	−14	9.7	8.2		⟨111⟩
TbSi	6.280	AF II	18	−33	9.52	7.9		⟨111⟩
TbS	?							
TbSe	5.741							
TbTe	6.101							
DyN	4.905	Ferro	17.6	20	10.5	7.4	9.3	⟨100⟩
DyP	5.654	HoP type	8	18	9.9	7.8	6.35	?
DyAs	5.803	HoP type	8.5	2	10.1	9.6	5.3	⟨100⟩
DySb	6.153	AF	9.5	−4	9.75	9.5	9.5	⟨100⟩
DyBi	6.251	AF II	11.2	−8	10.6	8.7	9.7	⟨100⟩
DyS	5.490				10.4			

(continued)

Table A1 (*continued*)

Compound	a (Å)	Magnetism	$T_{crit.}$ (K)	θ_{para} (K)	$\mu_{eff.}$ (μB)	$\mu_{neut.}$ (μB)	$\mu_{sat.}$ (μB)	Easy axis
DySe	5.711				10.4			
DyTe	6.075				10.5			
HoN	4.877	Ferri	13.3	12	10.8	8.9	9.9	⟨100⟩
HoP	5.626	HoP type	5.5	6	10.2	?	9.2	⟨100⟩
HpAs	5.771	AF II	4.8	1	10.35	8.8	9.5	⟨100⟩
HoSb	6.130	AF II	5.5	−2.5	10.8	9.3	9.3	⟨100⟩
HoBi	6.228	AF II	5.7	?	?	?	8.7	⟨100⟩
HoS	5.465	AF II	17.5/21	−15	10.3	7.4		
HoSe	5.680				10.6			
HoTe	6.049	AF II	20		10.5	7.6		⟨111⟩ or ⟨100⟩
ErN	4.836	Ferri	3.39	4	9.4	6	7.5	⊥⟨111⟩
ErP	5.606	AF II	2.2	1	9.3	5.7	8.5	⊥⟨111⟩
ErAs	5.745	AF	2.9	−2	9.6		8.4	
ErSb	6.107	AF	3.36	−3	9.8	7	7.3	⊥⟨111⟩
ErBi	6.202	AF	3.53	−6	9.4			
ErS	5.432	AF II	7.8/8.5		9.5	5.9		⟨111⟩
ErSe	5.662	AF II	9.5/10/11	−18	9.44	6.5		⟨111⟩
ErTe	6.021	AF			9.3	5.5		
TmN	4.809	n.o.		−18	7.6			
TmP	5.573	n.o.		−2	7.5			
TmAs	5.721	n.o.		−2	7.45			
TmSb	6.083	n.o.		−3	7.4			
TmBi	6.192	n.o.		12	?			
TmS	5.412	AF II ? 4*k*	5.17	10	7.0	3.4		⟨111⟩/⟨100⟩
TmSe	5.640	AF I	3.2	−29	6.39	1.7		⟨100⟩
TmTe	6.349	AF II	0.21	−5	5.22			⟨111⟩
YbN	4.785	AF III	0.73	−11.6	4.8	0.39		
YbP	5.555	AF II	0.64	−11.5	4.3	0.79/1.03 (Mössbauer/ neutrons)		
YbAs	5.702	AF III	0.49	−17	4.25	0.82/0.86 (Mössbauer/ neutrons)		
YbSb	6.079	no l.r.ord	0.32	−20	4.35	0.63		
YbBi								

[a] a = Lattice parameter; $\mu_{neut.}$ = neutron moment; TIP = temperature-independent paramagnetism; AF = antiferromagnetic (type I, IA, II, III); F = ferromagnetic.

Table A2
Magnetic properties of actinide monopnictides and monochalcogenides [a]

Compound	a (Å)	Magnetism	$T_{crit.}$ (K)	θ_{para} (K)	$\mu_{eff.}$ (μB)	$\mu_{neut.}$ (μB)	$\mu_{sat.}$ (μB)	Easy axis
UN	4.890	AF I	53		3.1	0.75		⟨100⟩
UP	5.588	AF I	125	13.5	3.2	1.7/1.9	0.53	⟨100⟩/⟨111⟩
UAs	5.768	AF I/IA	127/66	50	3.4	1.9/2.25	0.53	⟨100⟩/⟨111⟩
USb	6.209	AF I	214	169	3.8	2.85		⟨100⟩
UBi	6.363	AF	285	115	4.0	3.0		
US	4.897	F	178	180	2.3	1.7	1.55	⟨111⟩
USe	5.739	F	160	160	2.5	2.0	1.8	⟨111⟩
UTe	6.150	F	104	111	2.8	2.25	1.95	⟨111⟩
NpN	4.897	F	84	100	2.13	1.4		⟨111⟩
NpP	5.615	AF 3+3−	119/74	110	2.85		1.8/2.3	⟨100⟩
NpAs	5.835	AF 4+4−	175/142	184	2.82		1.74/2.5	⟨100⟩/⟨111⟩
NpSb	6.254	AF I	197	161	2.5			

(*continued*)

Table A2 (*continued*)

Compound	a (Å)	Magnetism	$T_{crit.}$ (K)	θ_{para} (K)	$\mu_{eff.}$ (μB)	$\mu_{neut.}$ (μB)	$\mu_{sat.}$ (μB)	Easy axis
NpBi	6.438		193					⟨100⟩
NpS	5.532	AF II	23	−150/81	1.9	0.7		⟨100⟩
NpSe	5.806	AF	38	−130	2.15	1.0		
NpTe	6.198	AF	30	−105	2.47			
PuN	4.905	AF	13		1.1			
PuP	5.550	F	130	125	0.97	0	0.6	⟨100⟩
PuAs	5.858	F	125		1.0		0.67	⟨100⟩
PuSb	6.241	AF/F	85/75		1.0	0/0.74	0/0.65	⟨100⟩
PuBi	6.358	AF	65		0.8		0.61	⟨100⟩
PuS	5.541	TIP						
PuSe	5.793	TIP						
PuTe	6.183	TIP						
AmN	4.995	TIP						
AmP	5.711	TIP						
AmAs	5.876	TIP(AF)						
AmSb	6.240	TIP						
AmBi	6.338	TIP						
AmS	5.595	?						
AmSe	5.821	?						
AmTe	6.171	TIP						
CmN	5.041	F	109		7.02			
CmP	5.743	F	73					
CmAs	5.905	F	88		6.58			
CmSb	6.243	F	162					
CmBi								
BkN		F	87					
CfN		F(?)	25		10.1			
CfP								
CfAs		AF	17.5		10.1			
CfSb		AF	25		10.3			
CfAs								
CfS								
CfSe								
CfTe								

[a] Notations as in Table A1.

References

[1] J.L. Smith and E.A. Kmetko, *J. Less-Common Met., 90* (1983) 83.

[2] H.R. Ott, F. Hulliger and Y.H. Rudigier, in P. Wachter and H. Boppart (eds.), *Valence Instabilities,* North-Holland, Amsterdam, 1982, p. 511.

[3] P. Wachter, F. Marabelli and B. Bucher, *Phys. Rev. B, 43* (1991) 11136.

[4] S.E. Nave, J.R. Moore, R.G. Haire, J.R. Peterson, D.A. Damien and P.G. Huray, *J. Less-Common Met., 121* (1986) 319.

[5] R.J. Birgenau, E. Bucher, J.P. Maita, L. Passell and K.C. Turberfield, *PHys. Rev. B, 8* (1973) 5345.

[6] G.H. Lander and W.G. Stirling, *Phys. Rev. B, 21* (1980) 436.

[7] W.J.L. Buyers, A.T. Murray, T.M. Holden, E.C. Svenson, P. de V. Du Plessis, G.H. Lander and O. Vogt, *Physica B, 102* (1980) 291.

[8] M. Escorne, A. Mauger, D. Ravot and J.C. Achart, *J. Appl. Phys., 55* (1984) 1835.

[9] O. Vogt and K. Mattenberger, in K.A. Gschneidner, Jr., L. Eyring, G.H. Lander and G.R. Choppin (eds.), *Handbook on the Physics and Chemistry of Rare Earths,* Vol. 17, North-Holland, Amsterdam, 1993, p. 301.

[10] G.T. Trammell, *Phys. Rev., 131* (1963) 932.

[11] B.R. Cooper, Q.G. Sheng, S.P. Lim, C. Sanchez-Castro, N. Kioussis and J.M. Wills, *J. Magn. Magn. Mater., 108* (1992) 10.

[12] J.P. Sanchez, J.C. Spirlet, J. Rebizant and O. Vogt, *J. Magn. Magn. Mater., 63–64* (1987) 139.

[13] J.P. Sanchez, P. Burlet, S. Quezel, D. Bonnisseau, J. Rossat-Mignod, J.C. Spirlet, J. Rebizant and O. Vogt, *Solid State Commun., 67* (1988) 999.

[14] O.R. Vogt and K. Mattenberger, *J. Less-Common Met., 133* (1987) 53.

[15] D.J. Lam, *AIP Conf. Proc., 5* (1972) 892.

[16] D.J. Lam, F.Y. Fradin and O.L. Kruger, *Phys. Rev., 187* (1969) 606.

[17] M. Haessler and C.H. de Novion, *J. Phys. C, 10* (1977) 589.

[18] K. Mattenberger, O. Vogt, J.C. Spirlet and J. Rebizant, *J. Less-Common Met., 121* (1986) 285.
[19] P. Junod, A. Menth and O. Vogt, *Phys. Kondens. Mater., 8* (1969) 323.
[20] S. Ozeki, Y.S. Kwon, Y. Haga, T. Suzuki, G. Kido and T. Kasuya, *Physica B, 169* (1991) 499.
[21] R.B. Beeken and J.W. Schweitzer, *Phys. Rev. B, 23* (1981) 3620.
[22] O. Vogt and B.R. Cooper, *J. Appl. Phys., 39* (1968) 1202.
[23] B.R. Cooper and O. Vogt, *Phys. Rev. B, 1* (1970) 1211.
[24] B.R. Cooper and O. Vogt, *Phys. Rev. B, 1* (1970) 1218.
[25] K. Mattenberger and O. Vogt, *Phys. Scr. T, 45* (1992) 103.
[26] F. Hulliger and H.R. Ott, *Z. Phys. B, 29* (1978) 47.
[27] Y.S. Kwon, Y. Haga, O. Nakamura, T. Suzuki and T. Kasuya, *Physica B, 171* (1991) 324.
[28] G. Busch, O. Marincek, A. Menth and O. Vogt, *Phys. Lett., 14* (1965) 262.
[29] G.A. Smolenskii, V.P. Zhuze, V.E. Adamyan and G.M. Loginov, *Phys. Status Solidi, 18* (1966) 873.
[30] G. Busch and O. Vogt, *Phys. Lett. A, 25* (1967) 449.
[31] B.R. Cooper, A. Furrer, W. Bührer and O. Vogt, *Solid State Commun., 11* (1972) 21.
[32] J. Rossat-Mignod, P. Burlet, S. Quezel, O. Vogt and H. Bartholin, in J.E. Crow, R.P. Guertin and T.W. Mihalisin (eds.), Crystalline Electric Field and Structural Effects in f-Electron Systems, Plenum Press, New York, 1982, p. 501.
[33] P.W. Anderson, *Phys. Rev., 79* (1950) 350.
[34] H.R. Child, M.K. Wilkinson, J.W. Cable, W.C. Koehler and E.O. Wollan, *Phys. Rev., 131* (1963) 922.
[35] J. Rossat-Mignod, P. Burlet, H. Bartholin, O. Vogt and R. Lagnier, *J. Phys. C, 13* (1980) 6381.
[36] J. Rossat-Mignod, G.H. Lander and P. Burlet, in A.J. Freeman and G.H. Lander (eds.), *Handbook on the Physics and Chemistry of the Actinides,* Vol. 1, North-Holland, Amsterdam, 1984, p. 415.
[37] P. Burlet, S. Quezel, J. Rossat-Mignod and R. Horyn, *Solid State Commun., 55* (1985) 1057.
[38] K. Mattenberger, O. Vogt, J. Rebizant, J.C. Spirlet, F. Bourdarot, P. Burlet, J. Rossat-Mignod, M.N. Bouillet and J.P. Sanchez, *J. Magn. Magn. Mater., 43* (1992) 104.